

Electron transport in a mesoscopic superconducting / ferromagnetic hybrid conductor

M. Giroud¹, K. Hasselbach¹, H. Courtois¹, D. Mailly² and B. Pannetier¹

¹ Centre de Recherches sur les Très Basses Températures - C.N.R.S. associated to Université Joseph Fourier, 25 Av. des Martyrs, 38042 Grenoble, France

² Laboratoire de Photonique et de Nanostructures, Route de Nozay, 91460 Marcoussis, France

February 1, 2008

Abstract. We present electrical transport experiments performed on submicron hybrid devices made of a ferromagnetic conductor (Co) and a superconducting (Al) electrode. The sample was patterned in order to separate the contributions of the Co conductor and of the Co-Al interface. We observed a strong influence of the Al electrode superconductivity on the resistance of the Co conductor. This effect is large only when the interface is highly transparent. We characterized the dependence of the observed resistance decrease on temperature, bias current and magnetic field. As the differential resistance of the ferromagnet exhibits a non-trivial asymmetry, we claim that the magnetic domain structure plays an important role in the electron transport properties of superconducting / ferromagnetic conductors.

PACS. 73.23.-b Electronic transport in mesoscopic systems – 74.80.Fp Point contacts; SN and SNS junctions – 72.25.-b Spin-polarized transport

1 Introduction

The question whether superconductivity can be induced in a ferromagnetic metal is of fundamental and practical importance. At the junction of a Ferromagnetic metal (F) with a Superconductor (S), the superconducting order parameter is predicted to oscillate and decay rapidly in the ferromagnet as the distance to the F/S interface increases. The natural length scale is the exchange length $L_{exch} = \sqrt{\hbar D / \mu_B H_{exch}}$, where D is the electron diffusion constant and H_{exch} the exchange field expressed in Tesla. The latter expression holds in the dirty limit $L_{exch} > l_e$, where l_e is the elastic diffusion length. Physically, these effects occur because of the wave vector difference between spin-up and spin-down electrons at the Fermi level [1, 2]. L_{exch} is the length over which the two electrons of an Andreev pair get a phase difference of π . Oscillating behaviors were recently detected in measurements of the density of states of a F/S junction [3] and in the Josephson supercurrent of a S/F/S junction [4]. These experiments involved F layers with a thickness of the order of the exchange diffusion length L_{exch} which was actually made rather large by choosing a ferromagnetic metal with a small exchange field H_{exch} . In conventional ferromagnetic transition metals (Co which is used here, Ni, Fe, ...), the exchange energy $\mu_B H_{exch}$ is large and greatly overcomes the thermal energy $k_B T$ at cryogenic temperatures. The corresponding exchange diffusion length L_{exch} is very small, of the order of a few nanometers.

Many recent experiments involved mesoscopic F/S junctions with a micron-scale ferromagnetic conductor made of Co or Ni. Surprisingly, large proximity effects were observed in the transport properties [5, 6, 7, 8] of the samples with a transparent interface. When compared to the conventional superconducting proximity effect occurring in non-magnetic metals, [9] this behavior suggests that the relevant length scale is much larger than the expected coherence length L_{exch} . In the case of interfaces with an intermediate or low transparency, the effect was shown to be restricted to the interface, and was described within an extended BTK model [10]. Nevertheless, it was surprising that the fit values of the parameter Z , which is directly related to the interface transparency, varied so little in comparison with the wide range of interface resistance.

Alternative explanations, ignoring the proximity superconductivity in the ferromagnetic metal, have been proposed. In the case of a transparent interface, the spin accumulation at the F/S junction [11, 12, 13] could contribute significantly to the anomalous transport properties, together with the Anisotropic Magneto-Resistance (AMR) [14]. Spin accumulation arises near a F/S interface because of the mismatch between the unpolarized pair current in S and spin-polarized single electron current in F. An excess population of minority-spin electrons therefore develops in F in the vicinity of the interface over a length scale set by the spin-flip diffusion length L_{sf} . Another relevant mechanism could be the competition between the fringe field of the ferromagnet and the diamagnetism of the supercon-

ducting electrode. This may result in an inhomogeneous magnetic field distribution and affect locally AMR and/or the Hall effect in the ferromagnet. The AMR stems from spin-orbit coupling in the ferromagnet and results in an anisotropy of the resistivity when the angle between the local magnetization and the current flow changes. This enables the observation of magnetization reversal processes in the resistance of small magnetic particles [15].

The microscopic mechanism inducing superconductivity in F close to the S interface is the Andreev reflection where an incident electron is reflected into a phase-correlated hole of the same spin. This is equivalent to creating an Andreev pair of electrons with opposite spins. Obviously, this process will be affected by the spin polarization of the ferromagnetic metal and will even disappear in the case of a fully-polarized metal [16,17,18]. In this respect, an open question is the role of the magnetic domain structure. Crossed Andreev reflections [19] may appear in F two magnetic domains with opposite magnetization [20]. In the case of a ferromagnet with an inhomogeneous magnetization, it was also proposed that the spin-triplet component of the superconducting wave function can have a strong amplitude [21,22]. Interestingly, this component should exhibit a slower spatial decay than the usual singlet component. This inhomogeneous magnetization hypothesis is relevant because of both the shape anisotropy of micro-fabricated structures and the effect of the diamagnetism of the S electrode.

These open questions show the need for further investigation of transport in a mesoscopic ferromagnetic conductor connected to a superconductor. Here, we report on transport measurements of submicron Co-Al hybrid structures. Compared to our previous experiments [7], we modified both sample dimensions and geometry to focus on transport properties in the ferromagnet itself, near the superconducting contact. We observed a large resistance drop in samples with a highly transparent interface. We studied the dependence of this effect with the temperature, the magnetic field and the bias current. Our main result is the observation of a resistance asymmetry between the two nominally identical branches of the Co wire.

2 Samples description

2.1 Fabrication

The samples geometry (see Fig. 1) was designed for measuring the ferromagnet resistance in proximity to the superconducting contact, with zero net current through the interface. The Al contact is deposited on a lateral Co "finger", rather than directly on top of the Co wire itself, in order to minimize spurious current density redistribution effects when Al becomes superconducting [23,13]. As there are evidences that the superconducting contact influences transport only in the vicinity of the interface, the Co strip length was chosen as short as possible, namely 400 nm.

The sample fabrication process was chosen as to keep F/S contact resistances as small as possible. We used a

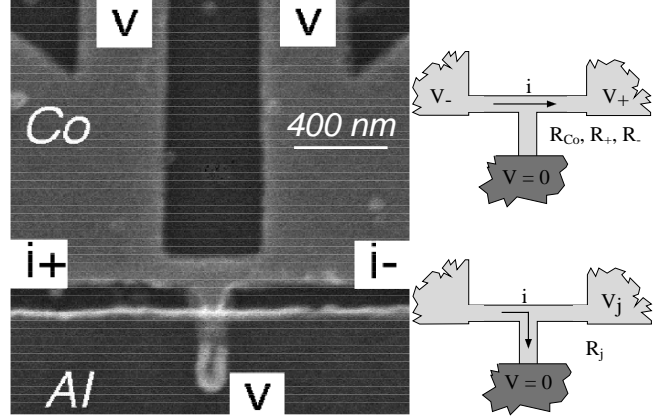


Fig. 1. Left : Micrograph of a typical sample made of a small T-shaped conductor embedded between two Co reservoir (right and left) and one Al electrode (bottom). The width and length of the small horizontal Co wire are respectively 120 nm and 400 nm. Right : schematics of the measurement wiring. The Co wire resistance R_{Co} is measured by applying the bias current between two ferromagnetic pads and measuring $V_+ - V_-$. The resistances R_+ and R_- of the right and left arms are accessed by measuring only V_+ or V_- . The junction resistance R_j is measured by applying the current from one Co reservoir to the Al electrode and measuring the voltage V_j of the opposite Co reservoir.

two-step lift-off process with in-situ Ar ion etch. Co was deposited first on the silicon substrate, in order to avoid step edges which could modify magnetization anisotropy and pin magnetic domain walls. A 50 nm layer of Co was e-beam evaporated at room temperature through a PMMA mask in a base vacuum below 10^{-7} mbar. An in-situ Ar ion milling of the Co surface was performed just before the 100 nm Al layer evaporation through the second PMMA mask.

2.2 Characterization

The deposition conditions together with the Co thickness are expected to result in an in-plane magnetization, which was confirmed by the AMR data. This orientation makes it easier to induce magnetization reversal under an applied magnetic field. The expected typical domain size is of the order of 100 nm, i.e. roughly comparable to the wire width. The Co resistivity was reproducibly high, in the $80 \mu\Omega\cdot\text{cm}$ range, whereas Al residual resistivity did not exceed $2 \mu\Omega\cdot\text{cm}$. This corresponds to an electron diffusive mean free path l_e of 1 nm in Co and 20 nm in Al. This also gives an estimated coherence length for superconducting correlations L_{exch} in Co of 3 nm. The Al superconducting coherence length and London penetration depth are of the order of $0.12 \mu\text{m}$ and $0.18 \mu\text{m}$ respectively. Overall, the Al resistive transition at $T_c \simeq 1.3$ K did not seem strongly affected by the proximity of the Co wire, except for a depressed critical current, roughly 3 times lower than for pure Al strips or microbridges of comparable dimensions.

We are mainly interested by the case of low resistance interfaces, as it is presumably the only case where the su-

perconductor has a strong influence on the ferromagnet. Interface resistance can be probed using two probes on the Al electrode and two probes at both ends of the Co strip. Due to the sample geometry, we can only measure a global resistance R_j which is the interface resistance in series with the Co lateral finger resistance and the Co spreading resistance. In the following, we consider experimental data collected on two samples (A and B) with a low resistance interface. The distance d between the main Co wire and the Al contact, i.e. the length of the lateral Co finger not covered by Al, was estimated from SEM micrographs to $d \simeq 50$ nm in sample A and $d \simeq 100$ nm in sample B. The global "junction" resistance R_j was about 17Ω in sample B. From the sample dimensions (see Fig. 1) and Co resistivity, we estimate that the Co finger itself is the main contribution. We can thus deduce that our interface specific resistance is below $6 m\Omega.\mu m^2$ in these samples with a transparent interface. For comparison, we also discuss data from one sample (C) with a degraded interface. The resistance R_j is 103Ω , which leads to an estimated interface specific resistance of $600 m\Omega.\mu m^2$.

3 Experimental results

3.1 Measurement procedure

We studied the electron transport properties of several samples down to a temperature of 30 mK. A magnetic field was applied in the sample plane, either parallel or perpendicular to the current in the Co wire. An experimental run with a field perpendicular to the substrate plane was also performed on some samples, to check that the Co AMR had the behavior expected for in-plane magnetization. In all our measurements, a d.c. current bias plus an a.c. current modulation below 100 nA were applied through the same contacts. Low-pass filters were inserted on the cryostat feedthroughs, as well as a d.c. rejection filter at the input of the lock-in amplifier. Depending on the wiring (see Fig. 1 right part), we investigated the resistance R_{Co} of the Co wire between the two reservoirs, that of one of the halves of this wire R_+ or R_- , or the junction resistance R_j .

3.2 Temperature dependence

Fig. 2 shows the temperature dependence of the Co conductor in samples A, B and C. As the temperature is decreased below the critical temperature of Al, the resistance of sample A first drops by about 1 %. It drops again by about 10 % below 0.2 K. Qualitatively similar results were obtained in other samples with a low resistance Co-Al interface. This is the case of sample B, which was patterned on the same wafer than sample A, but then the temperature of the large resistance drop is much higher whereas the first resistance drop just below 1.3 K is not so clearly visible. Therefore the characteristic temperature of the resistance drop, as well as the shape of the curve, appear to be sample-dependent. We do not yet know precisely which

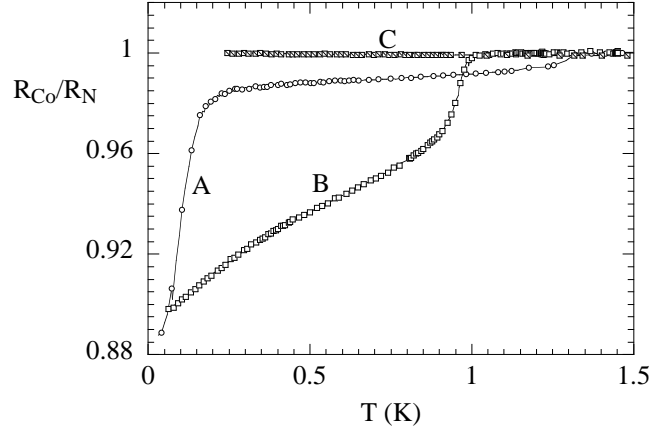


Fig. 2. Temperature dependence of the samples A, B and C Co wire resistance ratio after zero field cooling. The residual resistance of the Co wire at 1.5 K just above Al superconducting transition is 104Ω for sample A, 111Ω for sample B, 103.5Ω for sample C.

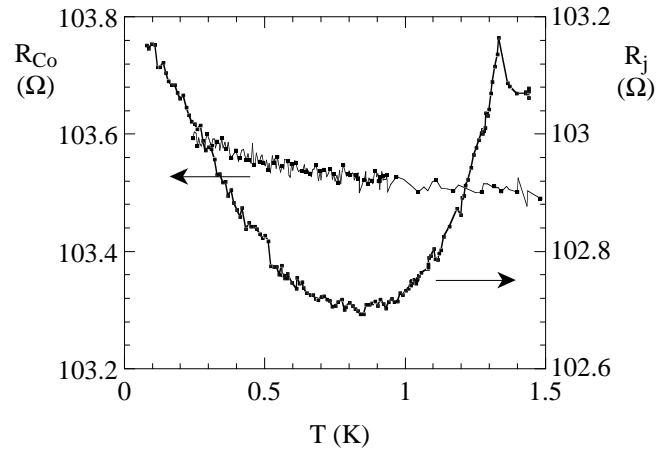


Fig. 3. Temperature dependence of Co wire resistance and Co-Al interface resistance in sample C. Note the difference in resistance change scale compared to Fig. 2.

factors monitor this variation. Let us point out that the total resistance drop magnitude is nearly 12 % in samples A and B. This effect is not observed at large bias current.

In the case of sample C with a poor interface transparency, the superconducting transition has almost no effect on the ferromagnet resistance R_{Co} , as shown in Fig. 2. It only weakly affects the junction resistance R_j , which first decreases of about 0.4 %, and then increases on cooling down (see Fig. 3).

3.3 Magnetoresistance

Fig. 4 shows the magneto-resistance of sample A at low bias current for a magnetic field applied in-plane along the Co wire, i.e. parallel to the current path. At low field ($H < 150$ mT), the magnetoresistance shows a small amplitude (less than 1 %) and a significant hysteresis. These two features suggest that this low-field behavior is due

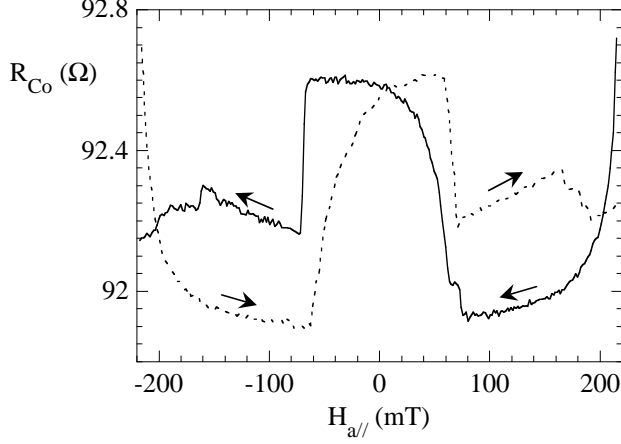


Fig. 4. Magneto-resistance of the Co wire in sample A. Magnetic field is applied parallel to the Co strip. The modulation current is 100 nA and the temperature 30 mK.

to Anisotropic Magneto-Resistance (AMR). The demagnetized multi-domain state reproducibly exhibits a larger resistance than the higher field state. The relatively sharp jumps at ± 70 mT are the signature of the cobalt coercive field $H_{coer.}$. In the high-field regime, we observe a large resistance increase up to the normal state residual resistance. This increase is the signature of the Al transition to the normal state at the Al superconducting critical field $H_{cS} \simeq 210$ mT.

Measurements on sample C (not shown) showed a small 0.6 % positive magneto-resistance when field and current are in-plane but perpendicular to each other. This anisotropy, as well as the amplitude of the resistance jumps, are consistent with the effect of the Co AMR in the case of an in-plane magnetization. The small resistance increase at very low temperature for sample C (see Fig. 3) can therefore be explained by a modification of the Co AMR induced by Al diamagnetic shielding.

Let us note a significant difference with our previous experiments [7] on 2 μm -long samples. In these long samples, magnetoresistance showed a smooth variation over a relatively broad field range. In the present short "T-shaped" samples, we reproducibly observe very well defined jumps at $\pm H_{coer.}$. This strongly suggests that our short wires contain a small number of domain walls which depin at this field, whereas long samples contain a larger number of domains walls, which will rotate or move along the sample in a broader field range.

3.4 Differential resistance

The differential resistance was investigated by superposing a d.c. current bias current to the a.c. modulation. Fig. 5 displays the total differential resistance measured in a standard four probes configuration between the "+" and the "-" ends of the Co wire. In sample A, we observe a resistance dip for current bias below 0.2 μA which mimics the resistance drop observed below 0.2 K. At this point, the voltage across sample A is about 20 μV , roughly a

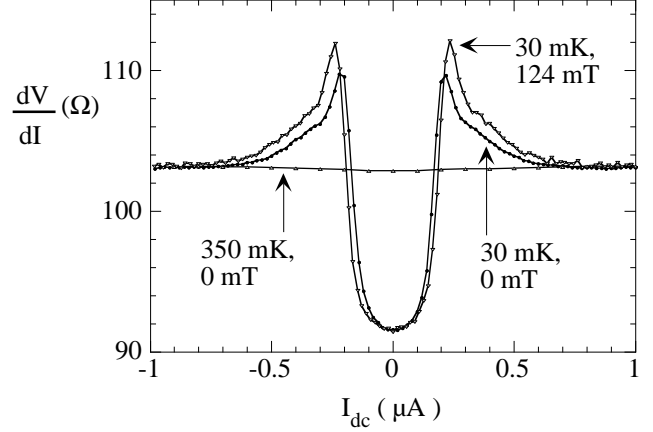


Fig. 5. Differential resistance dV/dI of sample A Co wire in various conditions : zero magnetic field, temperatures $T = 30$ mK and $T = 350$ mK ; magnetic field $H = 124$ mT, temperature $T = 30$ mK.

factor 10 below the expected Al gap. The high-bias resistance value coincides with the value obtained at high temperature, above the critical temperature of Al. The relative amplitude of the variation is in the 10 % range. A similar behavior was reproducibly observed in sample B and several other samples. The current range and the profile of the resistance dip appear to scale with the characteristic temperature of the resistance drop. No variation of the junction differential resistance was observed at low bias except for temperatures close to T_c .

Because of the relatively high resistivity of our Co film, we have to be careful about heating effects. At the lowest temperature (30 mK), we expect that the heat flow is essentially evacuated along the Co strip. At a temperature of 0.1 K, the thermal conductance of the Co strip, Co/Si interface, and Al strip, should be respectively about 100, 50 and 10 pW/K. The Joule power dissipated by the Co strip is only 4 pW at the 0.2 μA current bias required to suppress the resistance decrease. This means that at this bias the sample A cannot be heated above 0.1 K. We conclude that Joule heating is not sufficient to explain the differential resistance variation.

We also applied a ± 124 mT field along the Co strip, parallel to the current path. The value ± 124 mT was chosen as to be above the Co coercive field $H_{coer.} \simeq 70$ mT and below the Al superconducting critical field $H_{cS} \simeq 210$ mT. The Co conductor was therefore presumably close to magnetization saturation, although it may not yet be single domain. The current dependence of R_{Co} shown in Fig. 5 only shows a small difference compared to the zero field case. This difference is of the same order than the Co magnetoresistance jump at $H_{coer.}$, i.e. close to 1%.

3.5 Resistance asymmetry

We now come to our main result. Figure 6 top part shows sample A differential resistances of the left and right parts of the Co wire (R_+ and R_-), as well as the total resistance

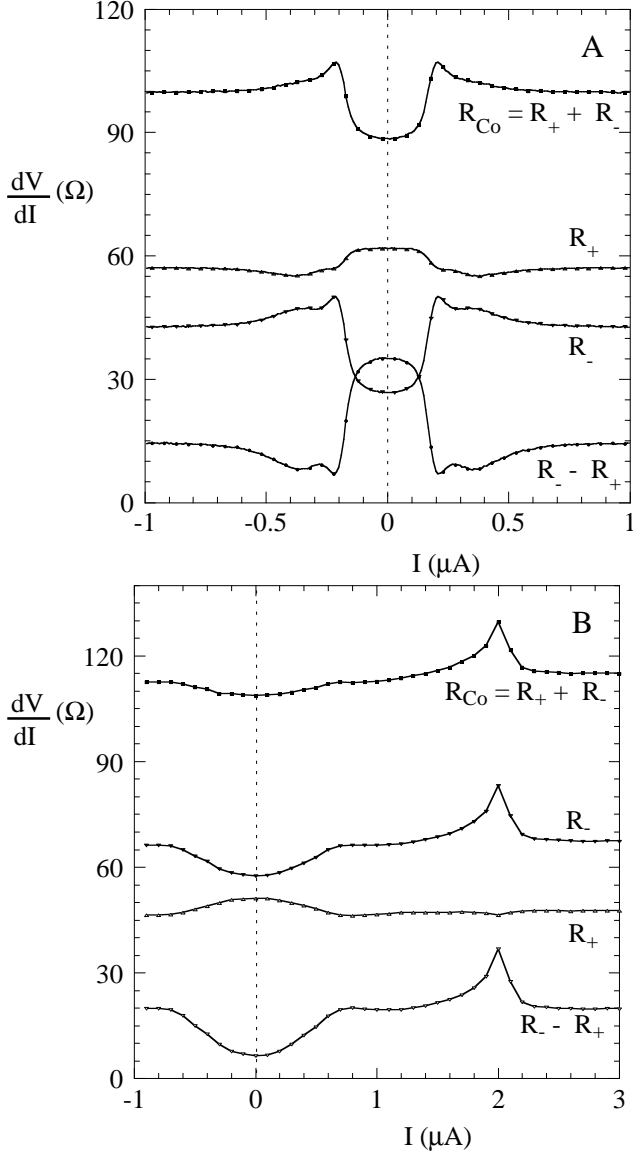


Fig. 6. Current bias dependence of the differential resistance of “+” and “-” parts of the Co wire in samples A (top) at $T = 30$ mK, and B (bottom) at $T = 700$ mK. In both cases, the sum of the two resistances R_+ and R_- matches the measured total resistance R .

$R_{Co} = R_- + R_+$ and the resistance difference $R_- - R_+$. The current path between the two ends of the Co strip remained unchanged, so that the net current through the interface is always zero. R_+ and R_- represents the differential resistance measured respectively with voltage probes at the “+” Co end and the Al contact, or between the Al contact and the “-” Co end (see Fig. 1).

We observe a non-trivial asymmetry between R_+ and R_- in the low bias regime. In the current range where Co resistance is depressed by the superconducting contact, R_- is lower and R_+ higher than its respective high-bias value. The relative variations $\Delta R_-/R_-$ and $\Delta R_+/R_+$ are significantly stronger (up to 35 %) than the total Co wire variation $\Delta R_{Co}/R_{Co}$ (about 12 %). At high bias, the dif-

ference between the values of R_+ and R_- may be explained by the inhomogeneities in the sample crystalline micro-structure. Let us note that the differential resistance remains symmetric with respect to the d.c. current bias, i.e. a current reversal produces a voltage sign reversal. Within a small experimental error, the sum of R_+ and R_- is always equal to the total differential resistance R_{Co} . Similar results were reproducibly observed on several samples, including sample B (Fig. 6 bottom).

4 Discussion of the results

First, let us comment on a difference between these results and our previous experiments [7]: we no longer observed a re-entrance of the metallic resistance. Here, the estimated Thouless energy of the Co conductor is $\epsilon_c = \hbar D/L^2 = 0.1K$, and a resistance minimum should have been observed close to 0.5 K, which is not the case. This contradicts the interpretation we proposed earlier, namely the occurrence of a re-entrant proximity effect in the resistance, similarly to the non-ferromagnetic metal case [9]. We come to the conclusion that the resistance minimum in our previous experiments may rather result from the competition between two opposite mechanisms: a resistance drop induced by the superconducting contact which we observe much more clearly in our shorter new samples, and a resistance upturn of different origin. Spin accumulation effects constitute an obvious candidate [13], but Anisotropic Magneto Resistance (AMR) cannot be excluded.

The first question we have to care about is whether the resistance drop is indeed occurring in the ferromagnet, or is merely a consequence of current redistribution in the superconducting short-circuit [23]. It is important to note that in our samples, the sheet resistance of Al above T_c is only 0.2Ω per square, which is much smaller than the sheet resistance of Co ($\simeq 20 \Omega$ per square). Even normal Al acts as a shunt. One can model our two-dimensionnal sample with an array of resistances of the order of the Co and Al sheet resistances. The result of this analysis is that the resistance drop expected at Al superconducting transition should not exceed the Al sheet resistance (0.2Ω). This is clearly much smaller than the experimental resistance drop, which exceeds 10Ω . It is also known that the AMR is of the order of only 1 to 2% in ferromagnetic 3d transition metals such as cobalt. We indeed observe this AMR effect in the low-field magnetoresistance (Fig. 4). Thus we are confident that the resistance drop observed in Co, about 10 % above the residual normal state case, is neither a trivial current redistribution effect in the superconducting short-circuit nor a simple AMR effect. The behavior of otherwise identical samples with respectively low or high junction resistance is so clearly distinct that we can conclude that interface transparency plays a key role. The comparison between Fig. 2 and 3 even shows that the sign of the resistance variation can be reversed, as was observed in Ref. [8]. In the case of a weakly transparent interface, our results are also compatible with the conclusion of Ref. [10] that no proximity effect appears in

the bulk of the ferromagnet. A significant influence from the superconductor on the ferromagnet occurs when the interface is transparent enough, and only in this case.

The differential resistance asymmetry when changing the voltage probes configuration is somewhat surprising since the sample were fabricated as symmetric. We have to consider physical phenomena which may contribute differently to the resistances R_+ and R_- of the two sample halves. From the sample geometry shown in Fig. 1, we see that R_+ and R_- may include a Hall effect contribution, related to the local field in the ferromagnet or to its magnetization (anomalous Hall effect) over the Co transverse dimensions (wire width plus finger length). The Hall voltage will contribute with opposite sign to R_+ and R_- , but should not contribute to the total resistance R_{Co} , as in this case voltage probes are aligned along the current lines. A d.c. current bias as low as $0.2 \mu\text{A}$ cannot significantly affect the magnetization and the domains structure [24,25], so that the Hall resistance should remain constant in the experimental bias range. Moreover, we observed that samples with a high resistance interface do not exhibit such a significant resistance asymmetry, although their magnetization and coercitive field are not significantly different. Therefore, the differential resistances and their asymmetry cannot be explained by the classical anomalous Hall effect in the ferromagnet, but are related to superconductivity.

In the interface region, electrons diffuse between Co and Al. In the case of a positive d.c. bias electrons coming from the "+" side have a higher energy than those going on the "-" side. An out-of-equilibrium energy distribution will develop near the interface even with a zero net current [9]. Because of the mismatch between spin-polarized current in F and unpolarized pair current in S, any current between S and F will be also associated to a non-equilibrium spin polarization, in a distance range from the interface determined by the spin flip diffusion length. This spin polarization is energy-dependent, should be maximum at zero bias and vanish above the superconducting gap. With this simple picture in mind, one might understand that $R_+(I)$ and $R_-(I)$ may be different at low bias. Nevertheless, we expect that $R_-(-I)$ should behave as $R_+(I)$ if the sample is symmetric. This is clearly not the case, one exhibiting a maximum at zero bias and the other one a minimum.

Therefore, the difference between R_+ and R_- must stem from a physical asymmetry in the sample itself, the most obviously possible one being the magnetic domains structure in an otherwise symmetric geometry. Since the T shape results in a complicated shape anisotropy, it is very likely that a non-symmetric magnetic domain structure is present in the central region of our sample. The amplitude and the sign of this asymmetry will be of course sample-dependent. If we assume that there is only a small number of domains in our short samples, and if the spin flip diffusion length is not much smaller than domain size (e.g. in the 200 nm range), the chemical potential drop may be different for electrons travelling from one Co contact (or the other) to the Al electrode, depending on the magnetic do-

main structure in the R_+ or R_- section of the cobalt wire. Nevertheless, the actual effect of the superconductivity on the electron transport in Co and the physical origin of the resistance drop remains undetermined. It could be a long-range superconducting proximity effect like the predicted long-range triplet component [21,22], spin accumulation effect in close relation with the sample geometry [12,13], or Andreev reflections of electrons of opposite spins in adjacent ferromagnetic domains of different magnetization [19,20].

5 Conclusion

In this work, we brought new experimental evidence for large resistance decrease in hybrid Ferromagnetic / Superconducting devices. This effect is clearly distinct from the Anisotropic MagnetoResistance (AMR) of smaller amplitude. A high interface transparency was found to be necessary for observing large effects. We suggest the relevance of the magnetic domain structure in the transport properties in the vicinity of a F/S contact. Further work on transport properties of F/S junctions with a high control of the magnetic domain structure is in progress.

We thank W. Belzig, R. Mélin and M. Viret for discussions and C. Veauvy for help in cryogeny. We acknowledge discussions within the "Dynamics of Superconducting Nanocircuits" TMR network and the "Mesoscopic Electronics" COST P5 action. This work is supported by the French Ministry of Education and Research under an ACI contract.

References

1. A.I. Larkin and Yu.N. Ovchinnikov, *Sov. Phys. JETP* **20**, 762 (1965) ; P. Fulde and R.A. Ferrel, *Phys. Rev.* **135**, A550 (1964).
2. E. A. Demler, G. B. Arnold and M. R. Beasley, *Phys. Rev. B* **55**, 15174 (1997).
3. T. Kontos, M. Aprili, J. Lesueur and X. Gison, *Phys. Rev. Lett.* **86**, 304 (2001).
4. V.V. Ryazanov, V.A. Oboznov, A.Yu. Rusanov, A.V. Veretennikov, A.A. Golubov and J. Aarts, *Phys. Rev. Lett.* **86**, 2427 (2001).
5. V. T. Petrashov, *JETP Lett.* **59**, 551 (1994).
6. M. D. Lawrence and N. Giordano, *J. Phys. Condens. Matter* **8**, 563 (1996).
7. M. Giroud, H. Courtois, K. Hasselbach, D. Mailly and B. Pannetier, *Phys. Rev. B* **58**, R11872 (1998).
8. V. T. Petrashov, I. A. Sosnin, I. Cox, A. Parsons and C. Troadec, *Phys. Rev. Lett.* **83**, 3281 (1999).
9. H. Courtois, P. Charlat, Ph. Gandit, D. Mailly and B. Pannetier, *J. of Low Temp. Phys.* **116**, 187 (1999).
10. J. Aumentado and V. Chandrasekar, *Phys. Rev. B* **64**, 054505 (2001).
11. F.J. Jedema, B.J. van Wees, B.H. Hoving, A.T. Filip and T.M. Klapwijk, *Phys. Rev. B* **60**, 16549 (1999).
12. V. I. Fal'ko, C. J. Lambert and A. F. Volkov, *JETP Lett.* **69**, 532 (1999).

13. W. Belzig, A. Brataas, Y.V. Nazarov and G.E.W. Bauer, *Phys. Rev. B* **62**, 9726 (2000).
14. U. Rüdiger, J. Yu, L. Thomas, S.S.P. Parkin and A.D. Kent, *Phys. Rev. B* **59**, 11914 (1999).
15. J. Aumentado and V. Chandrasekhar, *Appl. Phys. Lett.* **74**, 1898 (1999).
16. M.J.M. de Jong and C.W.J. Beenakker, *Phys. Rev. Lett.* **74**, 1657 (1995).
17. R.J. Soulen, J. Byers, , M.S. Osofky, B. Nadgorny, T. Ambrose, S.F. Cheng, P.R. Broussard, C.T. Tanaka, J. Nowack, J.S. Moodera, A. Barry and M.D. Coey, *Science* **282**, 5386 (1998).
18. S.K. Upadhyay, A. Palanisami, R.N. Louie and R.A. Buhrman, *Phys. Rev. Lett.* **81**, 3247 (1998).
19. G. Deutscher and D. Feinberg, *Appl. Phys. Lett.* **76**, 487 (2000).
20. R. Mélin, *Europhys. Lett.* **51**, 202 (2000).
21. F. S. Bergeret, A. F. Volkov and K. B. Efetov, *Phys. Rev. Lett.* **86**, 4096 (2001).
22. A. Kadigrobov, R.I. Skekhter and M. Jonson, *Europhys. Lett.* **54**, 394 (2001).
23. F.K. Wilhelm, A.D. Zaikin and H. Courtois, *Phys. Rev. Lett.* **80**, 4289 (1998).
24. M. Tsoi, A.G.M. Jansen, J. Bass, W.C. Chiang, M. Seck, V. Tsoi and P. Wyder, *Phys. Rev. Lett.* **80**, 4281 (1998).
25. J.E. Wegrowe, D. Kelly, X. Hoffer, P. Guittienne, and J.P. Ansermet, *J. Appl. Phys.* **89**, 7127 (2001).